ASSESSMENT OF A LASER SCANNING SYSTEM FOR DEFORMATION MEASUREMENTS

N. N. Al-Hanbali[1], S. El-Hakim[2], W. F. Teskey[3], R. S. Radovanovic[3], M. A. Chapman[4]

[1]Surveying and Geomatics Eng. Dept., Al-Balqa Applied University, Jordan,
nhanbali@index.com.jo
[2]Visual Information Technology, National Research Council of Canada,
Sabry.El-Hakim@nrc.ca.
[3]Geomatics Eng. Dept, Faculty of Engineering, The University of Calgary, Calgary, AB, Canada,
wteskey@ucalgary.ca., rsradova@ucalgary.ca
[4]Civil Engineering Department, Ryerson University, Toronto, ON, Canada,
mchapman@acs.ryerson.ca

KEY WORDS: Laser Scanning, Calibration, Digital Imaging, Accuracy, Industrial Metrology

ABSTRACT

The Laser Scanning System (LSS) is a leading-edge technology laser-based three-dimensional vision system. The LSS has the potential to be used for industrial metrology to produce fast and reliable three-dimensional information for machinery alignment monitoring applications. The goal of this paper is to asses and verify via lab testing the calibration procedure followed and the feasibility of using the LSS for monitoring three-dimensional deformations in close-range (±1.5 m) industrial applications. Two approached are presented in the paper as to asses the use of the LSS to measure three-dimensional movements in operating machinery. The first approach is based on using the LSS calibrated parameters to measure point movements, and the second one is based on using a local scaling approach to show deformation trends. The Lab test and on-site test results for both approached are summarized and discussed briefly in this paper. To achieve these goals, software were developed to provide the required tools to utilize the measuring system to produce good, reliable and precise results. The interface software to act as a link between the user's command from a PC-based machine and the LSS operating systems to be used for scanning and acquiring the required images is shown. The developed software for image analysis, processing, and digitization is also presented.

1. INTRODUCTION

In industrial metrology, machinery alignment monitoring need high deformation measurement precision (up to ±0.1mm), and instruments that has the capabilities to monitor deformations or misalignments continuously (Continuous monitoring), see Teskey et. al. (1994, 1995). In such applications, there is a limited space around the machinery, and hence, a single station setup instrument would be suitable. Another favorable feature is the use of a non-contact measurement instrument. Further more, it would be very useful to reconstruct surfaces and show deformation trends on these surfaces employing vision for such applications in addition to measure precisely point movements or misalignments.

The laser scanning technology has these capabilities and the potential to be utilized to show deformation trends on the surface of the machine as well as measure precisely point movements at any required position within the scanned field of view. Hence, the LSS has the potential to be used to monitor the thermal growth and the vibrations of operating machinery during startup or shutdown within such time interval.

In this paper the next section deals with the capabilities and basic geometry of the Laser Scanning System (LSS). The third section briefs the developed software and its functionality. Section four summarizes the conducted tests and the deformation measurement results of the local scaling approach.

Section five discusses the mathematical model and digital data interpretation for calibration purposes. The calibration approach used is based on least squares adjustment method using the unified approach, which integrates the constraint equations and weight constraints that are needed to stabilize the solution. Section six summarizes the calibration results

of the lab testing results, which proves that the system can measure deformations very precisely. The final section concluded the results of the testing presented to assess the use of the LSS for deformation measurements.

2. THE LASER SCANNING SYSTEM

The LSS technique is a dual-axis laser scanner based on an auto-synchronized triangulation scanning scheme that is patented to the National Research Council of Canada (NRC), NRC report(1993) and Rioux (1994). The system provides fast and reliable three-dimensional deformation measurements and can measure objects between 0.5 m to 100 m with a field of view of up of 36° X 40°, Beraldin et. al. (1992,1993). The system provides two output images: an intensity image and a depth coded image. The LSS can provide control over the scanned area and depth, which makes it a flexible system to use. For example, the operator can specify the image resolution, the scanned area within the maximum field of view, the suitable laser power for a specific surface, and the scanning mechanisms, Blais et. al. (1986, 1991) and Beraldin et. al. (1994). The system consists of a laser camera connected to a control panel, laser generator, and computer system running OS9 operating system, see Figure 1.

Figure 1: The Laser Scanning System

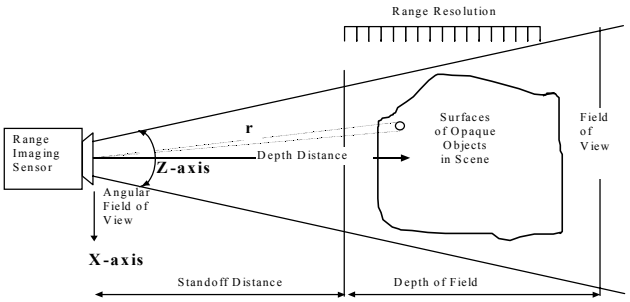

Figure 2: (a) Range imaging sensor with angular scan

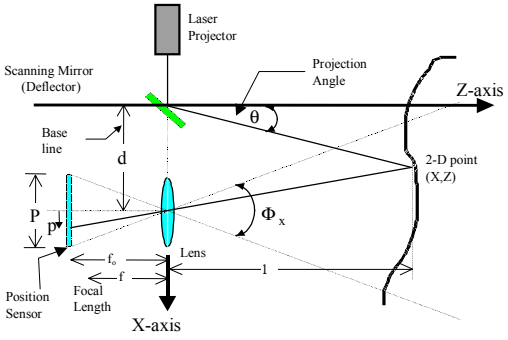

Figure 2: (b) Optical arrangement of the active triangulation principle

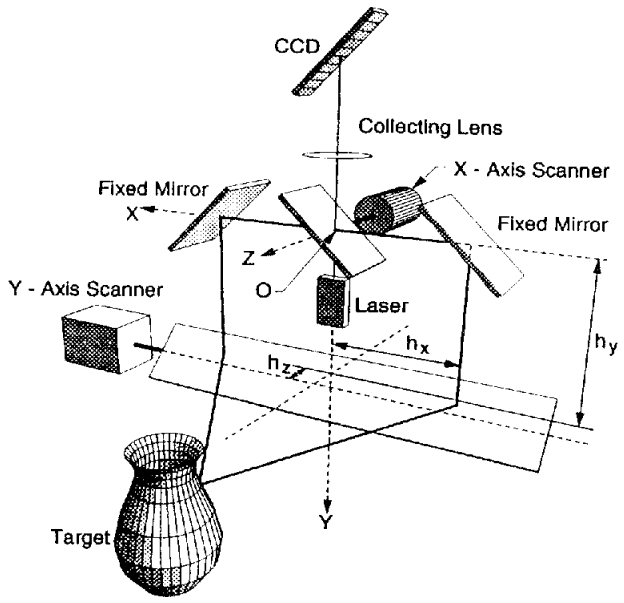

Figure 3: Dual-axis synchronized scanner in schematic representation (from Beraldin et. al., 1993).

The basic geometry of the scanner camera (range sensor) in two-dimensions is shown in Figure 2a, the scanned field of view, the detected depth distance r, and the angular field of view are also shown in the figure. Figure 2b illustrates the optical arrangement principle of a triangulation range-sensor and the projection of a scanned point on the position sensor of the laser camera.

The dual-axis-synchronized scanner, shown in Figure 3, is based on the Auto-synchronization approach and the Sheimpflug condition Rioux (1984). Auto-synchronization means that the projection of the laser spot and the deflection of the detection axis are synchronized automatically by using one rotating mirror and two fixed mirrors. The rotating mirror is silver-coated on both sides while the fixed mirrors are silver-coated on the front, Figure 3. For more information see Al-Hanbali (1998) and Al-Hanbali et. al. (1999).

The dual-axis laser scanner is shown schematically in Figure 3. Assuming that the scanner is set up (on a tripod for example) with the axis of the pulsed laser aligned vertically. The X-axis scanner (i.e., the galvanometer) measures the

angular position θ of a given point of interest in the horizontal plane, while the Y-axis scanner (i.e., galvanometer) measures the angular position ϕ of the same point in the vertical plane, or vise versa. As shown in the Figure, the distance to any point of interest is computed by triangulation. Two mirrors on either side of the Z-axis scanner act as a "**baseline**" and, as the scanning mirror (on the vertical axis between the two fixed mirrors) rotates, the position of the returning laser light on the CCD position detector shifts according to the distance from the point of interest.

The image can also be a single point image (field of view is 0° X 0°). The acquisition speed can be as high as 18 kHz. For example, a scene of 512X512 pixels can be captured, using the raster mode, in about 14 seconds. If only a small part of the scene is needed to be captured (e.g. vibration monitoring), using the Lissajous mode and 128 elements, the scan rate of the scene can be as high as 137 Hz., see Blais et. al.(1991) and Blais et. al.(1993).

3 DEVELOPED SOFTWARE

3.1 The Laser Scanner Interface Software:

A friendly user interface was especially developed for the LSS that runs under Windows NT and Windows 95/98 operating system, see Figure 4. The software acts as a link between the user's commands from a PC-based machine and the LSS operating system and is used for scanning and acquiring the required images, Al-Hanbali and Laurent (1995) and Al-Hanbali (1998).

The software handles various tasks. It sets and controls the various acquisition modes, image dimension and resolution, field of view and the various camera parameters, laser power, acquisition direction, focusing mode, and also controls the rotation stage speed and acceleration. The software also sets up and initializes the LSS, synchronizes and acquires images, and transfers, retrieves and saves images between the LSS and the PC-based machine.

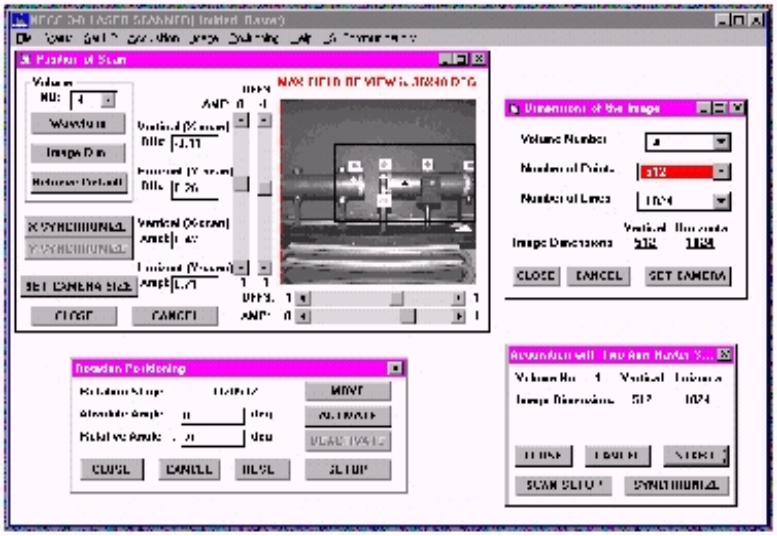

Figure 4: The interface software platform

3.2 Image Displaying, Processing and Digitization, Precise Edge Detection and Target Location and Surface Deformation representation Software:

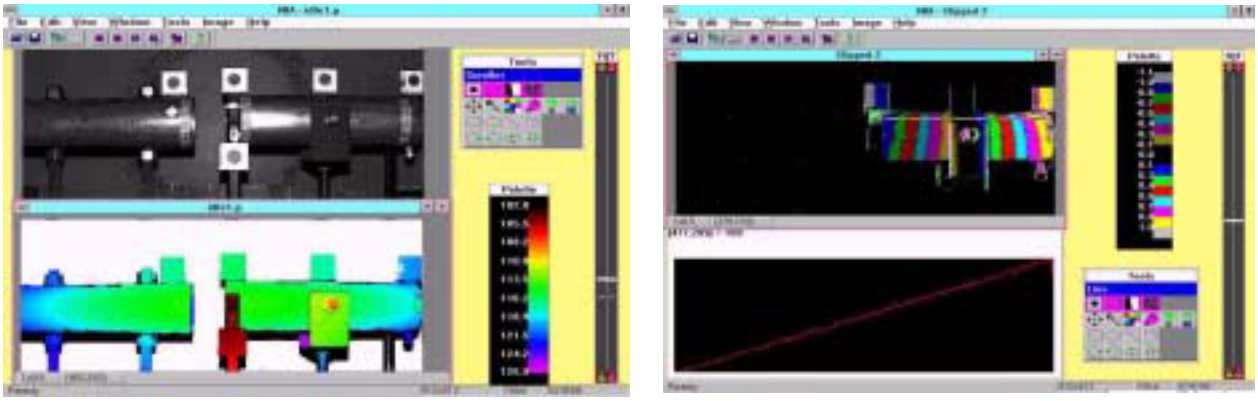

(a) (b)

Figure 5: (a) Platform of the image tools software: The intensity image and the depth coded image of the scanned mechanical test rig. (b) Platform of the image tools software: Introduced surface movement of the mechanical test rig.

Image processing techniques are well developed for conventional and CCD cameras. Due to the research environment, the author developed this software re-addressing image processing techniques and making use of the wide dynamic range of the LSS images (i.e. the digital pixel value of the LSS images is a two byte value), see Obidowski et. al. (1995). The software is used for the local scaling approach and for the calibration purposes. Figures 5a and 5b show some of the functionality of this software.

To illustrate the use of the software, Figure (5a) shows the top view of a typical industrial setup (Al-Hanbali 1994 and 1998). Figure (5a) shows the platform of the Image Tools software. The upper image is the intensity image displayed in gray values and the lower image is the depth-coded image. As shown in the color palette box, the colors represent scaled ranges (i.e. distances from the camera position to surface points in the scene). The upper right dialog box shows the different tools used to process laser images.

4 LOCAL SCALING APPROACH

4.1 Lab Testing:

To demonstrate the local scaling approach, a mechanical test rig shown in Figure 5 is scanned before and after introducing movement, producing for each case a depth coded image and an intensity image. Figure (5b) shows the result of scaling the direct difference between two depth-coded images. The upper left image in the Image Tools platform figure shows the surface movements displayed in colors. The movement values for each color are displayed in the color palette in centimeters. A profile of these movements along a cross-section is shown at the lower left side. For further details regarding the method see Al-Hanbali (1998).

The precision of measurements obtained from lab testing using this approach found to be equivalent to the expected precision of the LSS derived from the mathematical model for calibration purposes, (Al-Hanbali and Teskey 1994, Al-Hnbali 1998). Two test were conducted (one using a Static test rig and the other using Motorized test rig) applying approach. The precision of measured introduced movements were as follow: 0.2 mm for a depth distance of 0.75 m and 1.0 mm for a depth distance of 1.75 m. The expected precision of each are 0.15mm an d 0.85 mm, respectively.

4.2 On-Site Testing:

on-site test was carried out at the Sheerness Generating Station, Alberta, Canada. Figure 6 illustrates the machinery coupling of the turbine-generator combination, its intensity and depth coded images, a sphere mounted on a 2-d translation stage and sphere mapped image (mapping is done by NRC). The sphere and the retroreflective targets, shown in the figure, are used as reference points. The on-site testing was conducted in an environment of high temperature (about 40°C) and high vibration.

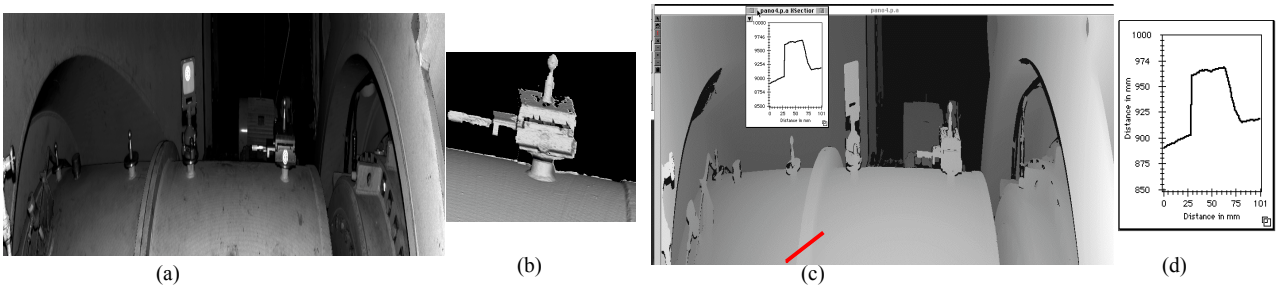

(a) (b) (c) (d)

Figure 6:(a) The machinery coupling, the retro-reflective targets and a sphere mounted on a 2-D translation stage. (b) Three-D mapping of the sphere and the translation stage. (c) Depth coded image of the machinery coupling, the retro-reflective targets and the 2-D translation stage. (d) The flange's approximate dimensions in millimeters.

Figure 7 shows the measurements and the RMS values of the intorduced movements of the sphere compared to the actual movements. Measurements are based on scaling two picked areas from the digital image. Area I is part of the sphere surface and area II is part of the surface of the 2-d translation stage (the moved part).

The achieved precision ranges from 0.20 mm when small deformation are introduced (up to 2.0 mm deformations) to 0.35 mm for large deformations (up to 50.0 mm deformations). The expected precision of the LSS derived from the mathematical model for calibration purposes is about 0.18 mm, see Al-Hanbali (1994) and Al-Hanbali and Luarent

(1995). Full details related to this case-study and how one should deal with refraction effects are given in Al-Hanbali (1998). The on-site test proves that the LSS can operate and provide reliable measurements under high temperature and vibration effects. Furthermore, the local scaling approach provides non-contact surface deformations is a simple and quick approach, and can be used reliably to show deformation trends on a surface of a machine or an object.

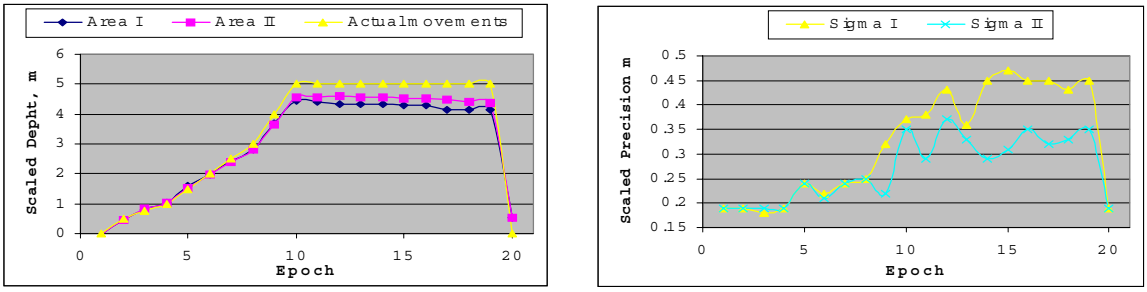

(a) (b)

Figure 7: Scaled measured depth distances and their corresponding precision compared to the actual introduced movements.

5 THE LSS MATHEMATICAL MODEL

4.1 Interpretation of Digital Values

Each point in the depth-coded image produced by the LSS is characterized by its pixel coordinates (**i** and **j**) and its registered value **p0** (that has a dynamic range between 0 and 32768). In a standard unit system (e.g. metric units), the **X**, **Y**, and **Z** coordinates of a point are functions of **p**, **θ** and **ϕ**, which are functions of the observations **p0**, **i**, and **j** where:

p = p0. scale_value , $\theta = \theta_0 + i \cdot \delta\theta$ and $\phi = \phi_0 + j \cdot \delta\phi$ Equation 1

where **θ** and **ϕ** are the X and Y-axes rotational angles, and the angles $\boldsymbol{\theta_0}$ and $\boldsymbol{\phi_0}$ are the initial angular field of view and **δθ** and **δϕ** are the step angles of the X and Y-axes of the mirrors. These variables are assumed to be constant for each LSS configuration (e.g. angular field of view, lens mode, acquisition strategy, image resolution, and/or other configurations). The intensity image is useful and provides better precision for detecting edges and locating target centers. Note that the pixel image coordinates are the same for both the depth-coded and the intensity images. For detailed explanation, see Al-Hanbali (1998) and Al-Hanbali et. al. (1999).

The distortion model used is based on a third order polynomial function with five distortion parameters. The polynomial functions absorb the distortion effects in the depth values p, the X-axis rotational angle **θ** and the Y-axis rotational angle **ϕ**.

4.2 The LSS Equations

The collinearity equations of the LSS are developed by NRC (Beraldin 1993, 1994). The equations are based on:

$$X_{LSS} = \lambda R_x(\mathrm{K}, \Phi, \omega)[X - X_0]_{OS} \quad \text{Equation 2}$$

$$Y_{LSS} = \lambda R_y(\mathrm{K}, \Phi, \omega)[Y - Y_0)]_{OS} \quad \text{Equation 3}$$

$$Z_{LSS} = \lambda R_z(\mathrm{K}, \Phi, \omega)[Z - Z_0)]_{OS} \quad \text{Equation 4}$$

where X_0, Y_0 and Z_0 are the 3-D coordinates of the LSS centre, and X, Y and Z are the 3-D coordinates of an object space point, both are in the object space coordinates system. The X_{LSS}, Y_{LSS} and Z_{LSS} are the 3-D coordinates of the object space point in the LSS coordinate system (correspond to LSS collinearity equations). Each is written as a function of the scale factor **λ**, the rotation matrix **R** between the object space coordinate system and the LSS coordinate system and the position of an object space point coordinates with respect to the LSS centre . The angle **λ** is the scale between the LSS coordinate system and the control field (target field) coordinate system. The value of the scale factor is assumed to be equal to one.

There are a total of twenty-two parameters to be solved for. These parameters consist of: two sensor parameters (related to the Pixel-Size and the Pixel-scale), nine internal parameters (related to the internal geometry of the scanner), four interior orientation parameters (θ_0, ϕ_0, $\delta\theta$, and $\delta\phi$), one scale factor and six exterior orientation parameters (X_0, Y_0, Z_0, ω, Φ, and K). For more details regarding the mathematical model, collinearity equations, distortion model, and the expected precision see Al-Hanbali (1998) and Al-Hanbali et. al. (1999).

5 THE CALIBRATION RESULTS

In imaging metrology, the calibration process of determining precisely the interior geometry of a camera is essential to produce accurate and reliable three-dimensional information from measurements made on two-dimensional imagery.

The observations of the LSS are used to define a three-dimensional object space scene or points based on the LSS interior orientation parameters and internal parameters. However, these coordinates are only defined with respect to the camera space coordinate system. To link the camera space coordinate system with the object space coordinate system, the exterior orientation parameters of LSS have to be determined and, hence, the object space datum is required. Special adjustment procedure with a suitable target field has been followed to determine a good set of calibrated parameters, see Al-Hanbali (1998 and 1999).

5.1 Precision of Absolute and Relative Measurements

Figure 8 shows the lab testing results to measure absolute and relative measurements, along the X-, Y- and Z- axes, at depth distances ranging from 0.65 m to 1.95 m. The RMS (root mean square) values of the relative coordinate measurements, are similar to the expected precision values calculated based on the variance values of the observations used in the least squares adjustment Al-Hanbali (1998 and 1999).

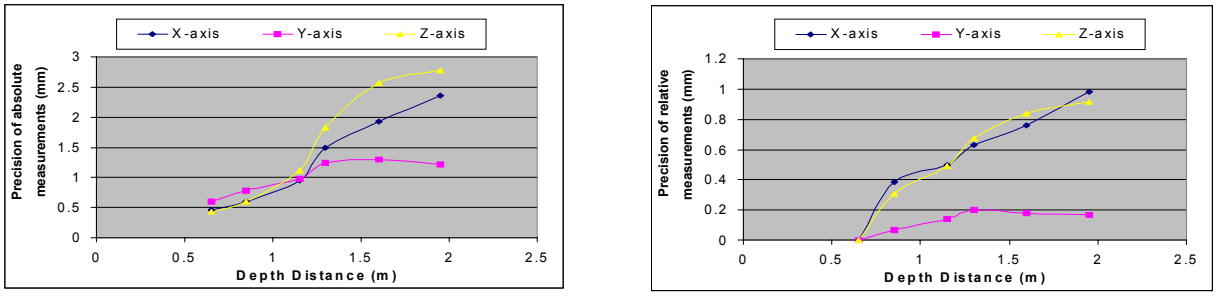

(a) (b)

Figure 8: The RMS values of the absolute and relative measurements at depth distances ranging from 0.65 m to 1.95 m.

The RMS values of the absolute measurements along the X-, Y- and Z-axes are nearly equal and similar in behavior, at depth distances less than 1.25 m. However, in the case of relative measurements, only the X-axis and the Z-axis are nearly similar and equal for depth distances that are less than 1.25 m. The Y-axis has better RMS values. This may indicate that most of the systematic errors of the Y-axis are eliminated. Finally, the accuracy of the relative measurements shows a drastic improvement in comparison to the accuracy of the absolute measurements.

5.2 Precision of Deformation Measurements

Figure 9 shows the deformation errors along X, Y and Z-axes. The errors are the difference between introduced movements of targets mounted on translation stage ditributed over the field of view of the LSS. The movements are calculated based on the calibrated parameters. The RMS values of the errors for a depth distance of 1.2 metre (Figure 8a) are: ±0.023 mm, ±0.074 mm, and ±0.041 mm along the X-, Y- and Z-axes, respectively. The RMS values of the errors for a depth distance of 1.5 metre (Figure 8b) are: ±0.032 mm, ±0.125 mm, and ±0.092 mm along the X-, Y- and Z-axes, respectively.

The movements for the depth distance of 1.2 m are introduced ranging from 0.25mm for the first epoch up to to 25 mm for epoch 10 (Figure 9a). Similarly, the movements for the depth distance of 1.5 m are introduced ranging from 0.25mm for the first epoch up to 50 mm for epoch 10 (Figure 9b). The absolute and relative measurement results, using calibrated parameters, show that the LSS has better RMS values and mean errors for the calibrated depth distances

(between 0.6 m and 1.25 m). Also, the relative measurements are more accurate than the absolute measurements. This is important since relative measurements are normally used.

The deformation measurement results show that the calibrated parameters can be used to provide results suitable for industrial applications in which required precision for movements are in the order of 0.1 mm.

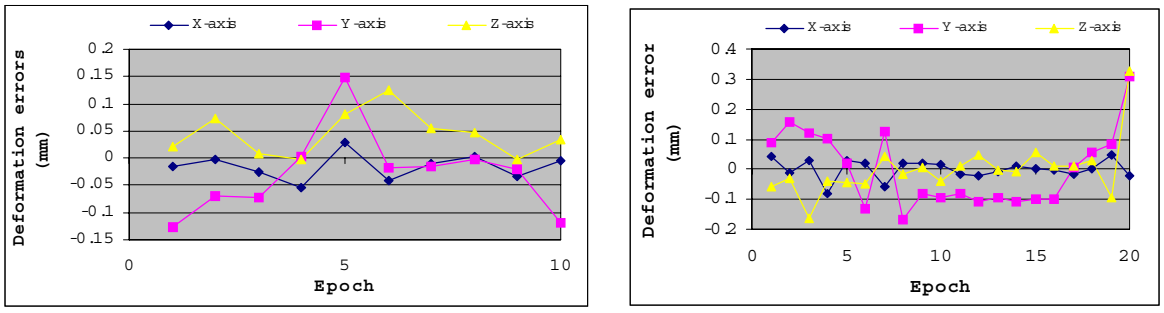

(a) (b)

Figure 9: The X, Y and Z axes deformation errors calculated based on the calibrated parameters due to the introduced movements along the Y and Z axes at a depth distance of 1.2 m and 1.5m.

5 CONCLUSION

The local scaling approach can be used satisfactorily since measured precision is approximately equal to the expected precision of the LSS derived from the mathematical model for calibration purposes, Al-Hanbali (1998). Thus, deformations trends on a surface can be extracted and illustrated reliably and precisely using the local scaling approach, which is a simple and a quick procedure.

The calibrated testing results show that the LSS system has better RMS values and mean errors for depth distances ranging from 0.6 meters up to 1.25 meters, Al-Hanbali (1998). Also, the relative measurements are more accurate than the absolute measurements, which is logical and it is important to be verified.

The assessment proves that for depth distances less than 1.5 m, the LSS provides reliable and precise measurements. Furthermore, this demonstrates that the LSS deformation measurement precision can be satisfactorily implemented in industrial applications (i.e. 0.1 mm precision), thereby achieving the major objective of the DAP research.

ACKNOWLEDGEMENT

This paper is the result of a research project named ***The Dynamic Alignment Project***. The motivation behind using the Laser Scanning System (LSS) is to develop a fast, non-contact measurement method for dynamic deformation monitoring. This development may complement and/or replace the state-of-the-art surveying engineering methods using electronic theodolite or electronic total station systems.

The Dynamic Alignment Project (**DAP**), which provided the financial support for my research work, is a collaborative research and Development project involving the department of Geomatics Engineering at The University of Calgary, the Natural Science and Engineering Research Council of Canada (**NSERC**), the National Research Council of Canada (**NRC**), and a number of large industrial firms in Western Canada. The principle collaborating industrial partner is Kadon Electro Mechanical Services Ltd. of Calgary. The funding provided through the **DAP** by **NSERC**, **Kadon**, and the other industrial partners is gratefully acknowledged.

I would like to thank the Visual Information Technology Group at the National Research Council Canada, for their support while I worked as a guest researcher. Special thanks and appreciation to Mr. Jacques Domey and to Mr. Marc Rioux, and also, to Luc Cournoyer, J.-Angelo Beraldin, and François Blais who supported me and answered my questions related to the Laser Scanning System technology. Furthermore, Luc Cournoyer helped us by providing his technical support and assistance to perform the lab tests (at The NRC labs) and the on-site test (at the Sheerness Generating Station) using the NRC laser scanner and his help is appreciated.

REFERENCES

Al-Hanbali, N. N. (1994). "Demonstration: Laser Scanning System," The Second Workshop of the Dynamic Alignment Project, Dept. of Geomatics Eng., The University of Calgary, Calgary, Alberta, November 18, 3pp.

Al-Hanbali, N. N., and Teskey, W. F. (1994). "Three-Dimensional Dynamic Deformation Monitoring using a Laser Scanning System," SPIE Conference, Videometrics III, Boston, Massachusetts, November 2-4, Vol. 2350, pp. 83-92.

Al-Hanbali, N. N. and N. St. Laurent (1995). "Demonstration: Laser Scanning System," The Third Workshop of the Dynamic Alignment Project, Dept. of Geomatics Eng., The University of Calgary, Calgary, Alberta, November 18, 3pp.

Al-Hanbali, N. N. (1998) "Assessment of a Laser Scanning System for Deformation Monitoring Applications," Ph.D. Thesis, 214 pp., Department of Geomatics Engineering, The University of Calgary, Calgary, 1998.

Al-Hanbali, N. N., S. El-Hakim, W.F. Teskey, M. A. Chapman, J, A-Beraldin, R.S. Radovanovic, M. R. Resheidat, (1999), " Calibration and Testing Results of a Laser Scanning System for Deformation Measurements", CMSC99 (Coordinate Measurement Systems Committee) Conference, Seattle, July 26-30, pp18

Beraldin, J.-A., Baribeau, R., Rioux, M., Blais, F. and Godin, G. (1992). "Model-Based Calibration of a Range Camera," Proceedings of the Eleventh IAPR International Conference on Pattern Recognition, The Hague, The Netherlands, August 30-September 3, pp. 167-193.

Beraldin, J.-A., El-Hakim, S. F. and Cournoyor, L. (1993). "Practical Range Camera Calibration," SPIE Conference, Videometrics II, Boston, Massachusetts, September 9-10, Vol. 2067, pp. 21-31.

Beraldin, J.-A., Rioux, M., Blais, F., Godin, G. and Baribeau, R. (1994). "Calibration of an Auto-synchronized Range Camera with Oblique Planes and Collinearity Equation Fitting," NRC Report, ERB-1041, National Research Council of Canada, Institute for Information Technology, Ottawa, Ontario, November, 25pp.

Blais, B., Rioux, M. and Maclean, S. G. (1991). "Intelligent, Variable Resolution Laser Scanner for the Space Vision System," Proceedings of the International Society for Optical Engineering (SPIE), Orlando, Florida, April 3-5, Vol. 1482, pp. 473-479.

Blais, F., Beraldin, J.-A., Rioux, M., Couvillon, R. A. and Maclean, S. G. (1993). "Development of a Real-Time Tracking Laser Range Scanner for Space Applications," Workshop on Computer Vision for Space Applications, Antibes, France, September 22-24, pp. 161-171.

NRC, Institute for Information Technology, Annual Report 1993/1994, National Research Council of Canada, Ottawa, Canada, ISSN 1183-9082.

Obidowski, R. M., Teskey, W. F., and Gaidadjiev R. (1995). "Integration of Sensors with Videometry for industrial Machinery Monitoring SPIE Conference, Videometrics IV, Philadelphia, Pennsylvania, October 23-26, Vol. 2598, pp. 295-304.

Rioux, M. (1984). "Laser Range Finder Based on Synchronized Scanners," Applied Optics, November, Vol. 23, No. 21, pp. 3837-3844.

Teskey, W. F., Obidowski, R. M. and Al-Hanbali. N. N. (1994). "Measurements of Machinery Deformations by High-Precision Survey methods," Journal of Surveying and Land Information Systems, Vo.54, No.1, pp. 1-10.

Teskey, W.F., Lovse, J.W., and Al-Hanbali, N.N. (1995), Deformation, Alignment and Vibration in a Large Turbine-Generator Set, Journal of Surveying Engineering, Vol. 122, No. 2, pp. 65-79.